This is the pre-peer reviewed version of the following article: Lu, H., et al. "Type III secretion-dependent and -independent phenotypes caused by Ralstonia solanacearum in Arabidopsis roots" in Molecular plant-microbe interactions, posted online 2 oct. 2017, which has been published in final form at DOI 10.1094/MPMI-05-17-0109-FI.

Type III secretion-dependent and -independent phenotypes caused by *Ralstonia solanacearum* in Arabidopsis roots

Haibin Lu[1☯#], Saul Lema A.[1☯], Marc Planas-Marquès[1☯], Alejandro Alonso-Díaz[1], Marc Valls[1,2,*] & Núria S. Coll[1*]

[1] Centre for Research in Agricultural Genomics (CSIC-IRTA-UAB-UB), Bellaterra, Catalonia, Spain

[2] Genetics Department, Universitat de Barcelona, Barcelona, Catalonia, Spain

☯ These authors contributed equally to this work

[#] Current address: State Key Laboratory of Crop Stress Biology for Arid Areas and College of Agronomy, Northwest A&F University, No.3 Taicheng Road, Yangling, Shaanxi, China. 712100.

* Address correspondence to: marcvalls@ub.edu, nuria.sanchez-coll@cragenomica.es

RUNNING TITLE

R. solanacearum root phenotypes in Arabidopsis

Word count (main body): 4,923

Number of figures: 6 figures (All are color)

Supplementary data: Table S1; Figures S1, S2, S3, S4, and S5,

Abstract

The causing agent of bacterial wilt, *Ralstonia solanacearum*, is a soilborne pathogen that invades plants through their roots, traversing many tissue layers until it reaches the xylem, where it multiplies and causes plant collapse. The effects of *R. solanacearum* infection are devastating and no effective approach to fight the disease is so far available. The early steps of infection, essential for colonization, as well as the early plant defense responses, remain mostly unknown.

Here, we have set up a simple in vitro Arabidopsis-*R. solanacearum* pathosystem that has allowed us to identify three clear root phenotypes specifically associated to the early stages of infection: root growth inhibition, root hair formation and root tip cell death.

Using this method we have been able to differentiate on Arabidopsis plants the phenotypes caused by mutants in the key bacterial virulence regulators *hrpB* and *hrpG*, which remained indistinguishable using the classical soil drench inoculation pathogenicity assays. In addition, we have revealed the previously unknown involvement of auxins in the root rearrangements caused by *R. solanacearum* infection.

Our system provides an easy to use, high-throughput tool to study *R. solanacearum* aggressiveness. Furthermore, the observed phenotypes may allow the identification of bacterial virulence determinants and could even be used to screen for novel forms of early plant resistance to bacterial wilt.

Key words (up to 10): *Arabidopsis thaliana*, bacterial wilt, cell death, in vitro pathosystem, *Ralstonia solanacearum*, root hair, root growth

Introduction

The soilborne phytopathogen *Ralstonia solanacearum* is the causing agent of bacterial wilt, one of the most destructive bacterial crop diseases worldwide (Hayward, 1991; Mansfield *et al.*, 2012). Also referred as the *R. solanacearum* species complex because of its wide phylogenetic diversity, this bacterium can cause disease on more than 200 plant species including many important economical crops (Genin & Denny, 2012). *R. solanacearum* accesses the plant through the root and traverses many root layers until it reaches the xylem, where it profusely multiplies. From there, it spreads through the aerial part and causes wilting of the stem and leaves (Genin, 2010).

Wilting symptoms caused by *R. solanacearum* are largely dependent on the presence of a functional type III secretion system (T3SS) (Boucher *et al.*, 1985). The T3SS is a needle-like structure present in many pathogenic bacteria that allows secretion of virulence proteins –called effectors- into the host cells (Hueck, 1998; Galan & Collmer, 1999). In plant-associated bacteria, the genes responsible for the regulation and assembly of the T3SS are known as *hypersensitive response and pathogenicity* (*hrp*) genes (Lindgren *et. al.,* 1986*)*. Transcription of the *hrp* genes and their related effectors is activated by HrpB, the downstream regulator of a well-described regulatory cascade induced by contact with the plant cell wall (Brito *et al.*, 2002). The cascade includes the membrane receptor PrhA, the signal transducer PrhI and the transcriptional regulators PrhJ and HrpG (Brito *et al.*, 2002). HrpG is downstream of PrhJ and directly controls HrpB expression (and thus expression of the T3SS genes) but it also activates a number of HrpB-independent virulence determinants such as genes for ethylene synthesis (Valls *et al.*, 2006).

Since the establishment of the *R. solanacearum* pathosystem almost two decades ago, leaf wilting has been typically used as the major readout to study the *Arabidopsis thaliana-R. solanacearum* interactions (Deslandes *et al.*, 1998). Soil drenching with a bacterial suspension followed by leaf symptom evaluation over a time course constitutes a solid measure to quantify the degree of resistance/susceptibility of the plant towards the pathogen. The disadvantages of this system are the uncontrolled influence of soil microbiota and its high variability due to infection stochasticity, as shown in potato (Cruz *et al.*, 2014). In addition, leaf wilting is the last step of *R. solanacearum* infection and does not provide information about early steps of colonization. Furthermore, soil opacity hinders direct observation of any morphological changes associated to bacterial invasion of plant tissues.

The establishment of gnotobiotic assays in which *R. solanacearum* is inoculated on plants grown axenically has opened the door to study the early steps of infection. *R. solanacearum* in vitro inoculation assays have been successfully established for tomato (Vasse *et al.*, 1995), petunia (Zolobowska & Van Gijsegem, 2006) and the model plants *Medicago truncatula* (Vailleau *et al.*, 2007) and *Arabidopsis thaliana* (Digonnet *et al.*, 2012). These studies have shed light on some common, as well as species-specific root phenomena associated to *R. solanacearum* infection. Reduced primary root elongation after infection is a common feature observed in all species analyzed. Other common root phenotypes that appeared after infection were swelling of the root tip (in tomato, petunia and *M. truncatula*), inhibition of lateral root growth (in petunia and Arabidopsis) and cell death (in *M. truncatula* and Arabidopsis). In petunia, *R. solanacearum* infection resulted as well in the formation of root lateral structures (Zolobowska & Van Gijsegem, 2006). These structures resembled prematurely terminated lateral roots, were present both in resistant and susceptible lines, and were efficient colonization sites.

In vitro pathosystems have helped defining the different stages of *R. solanacearum* infection. The bacterium was found to gain access into the tomato root through wound sites or natural openings such as emerging lateral roots (Vasse *et al.*, 1995; Saile *et al.*, 1997). In *M. truncatula* and Arabidopsis the bacteria can also enter intact roots through the root apex (Vailleau *et al.*, 2007; Digonnet *et al.*, 2012). In petunia it was shown that penetration occurs equally in resistant or susceptible plants (Zolobowska & Van Gijsegem, 2006). The second stage of infection involves invasion of the root cortical area. In this stage *R. solanacearum* quickly transverses the root cylinder centripetally via intercellular spaces, directed to the vasculature (Vasse *et al.*, 1995; Digonnet *et al.*, 2012). Massive cortical cell degeneration can be observed during this phase. The fact that cells not directly in contact with the bacteria also die led to propose that certain cell wall fragments degraded by *R. solanacearum* may act as signals to induce plant programmed cell death (Digonnet *et al.*, 2012). During the third stage of infection *R. solanaceraum* enters into the vascular cylinder and colonizes the xylem. In Arabidopsis, it was shown that vascular invasion is promoted by collapse of two xylem pericycle cells (Digonnet *et al.*, 2012). Once inside the xylem, bacteria start proliferating and moving between adjacent vessels by degrading the cell walls, but remain confined in the xylem. In the last stage of infection, disease symptoms become apparent at the whole organism level, as the stem and leaves start wilting.

All these studies have significantly broadened our understanding of the root invasion process. However, the molecular mechanisms that control these phenotypes and their timing remain vastly unexplored. In addition, no clear correlation has been established between any of the observed phenotypes and the host's resistance or susceptibility to *R. solanacearum*. Here, we have set up a simple in vitro pathosystem to determine the impact of *R. solanacearum* on Arabidopsis root morphology at the first stages of infection.

Results

In vitro infection with *R. solanacearum* causes a triple phenotype on Arabidopsis roots

In order to analyze the impact of *R. solanacearum* infection on Arabidopsis root morphology, we established a simple in vitro inoculation assay. Sterile seeds were sown on MS media plates and grown vertically for 7 days so that plant roots developed at the surface of the medium and could be easily inoculated and visualized. Plantlets were then inoculated 1 cm above the root tip with 5 µl of a solution containing *R. solanacearum.* Infection with the wild-type GMI1000 strain caused root growth arrest (Fig. 1A). To determine whether this effect depended on the inoculation point, we inoculated at the top, middle and tip of the root. As shown in Fig. S1, *R. solanacearum* causes root growth inhibition regardless of the infection point. Hence, all experiments were performed inoculating 1 cm above the root tip. Interestingly, along with root growth inhibition we observed two additional root phenotypes caused by *R. solanacearum* infection: production of root hairs at the root tip maturation zone (Fig. 1B), and cell death at the root tip. Cell death was visualized as either Evans blue (Fig. 1C) or propidium iodide staining (Fig. S2), both of them commonly used as cell death markers as they are excluded from living cells by the plasma membrane (Gaff & Okong'O-gola, 1971; Curtis & Hays, 2007).

R. solanacearum hrp mutants are altered in their capacity to cause the triple root phenotype

With these three phenotypes in hand we set out to identify their causative bacterial genetic determinants. For this, we analyzed the triple root phenotypes on plants

inoculated with *R. solanacearum* GMI1000 carrying mutations on the master regulators of virulence HrpG and HrpB. Bacteria bearing a disrupted *hrpG* lost the ability to inhibit root growth, but not those bearing disrupted *hrpB* versions (*hrpB* and *hrpBΩ*, figure 2a). Inoculation with the *ΔhrpG,* in which the whole ORF had been deleted, and its complemented strain *ΔhrpG(hrpG)* confirmed the requirement of HrpG but not HrpB to induce the phenotypes. Similarly, bacterial strains disrupted in the membrane receptor *prhA*, the signal transducer *prhI* and, to a lesser extent, the transcriptional regulator *prhJ* were all strongly affected in their capacity to inhibit root growth (Fig. 3). This is logical, since all these mutants show decreased *hrpG* transcription (Brito *et al.*, 2002). *hrp* mutants are all non-pathogenic (Boucher *et al.*, 1985), so the key role of HrpG in root inhibition compared to HrpB could be due to the fact that HrpG controls a larger number of bacterial virulence activities that have been proposed to be required for xylem colonization (Vasse *et al.*, 2000; Valls *et al.*, 2006). To check if root phenotypes correlated with bacterial colonization, 4-week-old Arabidopsis Col-0 plants were inoculated with the wild type *R. solanacearum* GMI1000 or its *hrpB* and *hrpG* deletion mutant counterparts. Bacterial loads were measured in aerial tissues of inoculated Arabidopsis plants 14 days after inoculation as colony forming units (CFUs) per gram of tissue. Fig. S3 shows that the capacity to colonize Arabidopsis plants of *hrpB* is significantly higher than of *hrpG* mutants. Thus, although *hrp* mutants had been already described to multiply *in planta* (Hanemian *et. al.,* 2013), HrpG seems to be more essential than HrpB for the bacterium to colonize the plant xylem and reach the aerial tissues.

Finally, we also observed that mutations in the *hrpB* and the *hrpG* regulators abolished root hair formation and cell death caused by *R. solanacearum* on roots (figure 2b and 2c). In summary, we proved that root hair production and cell death induction are T3SS-dependent phenotypes. In contrast, root growth inhibition, for which HrpG is required, does not depend on a functional T3SS.

R. solanacearum strains unable to cause the triple root phenotype are non-virulent on Arabidopsis

Our next goal was to determine whether the ability to cause the triple phenotype in Arabidopsis roots was conserved across different *R. solanacearum* strains and if there was a correlation to aggressiveness. For this, we inoculated in vitro-grown Arabidopsis Col-0 roots with *R. solanacearum* strains belonging to different phylotypes: our

reference strain GMI1000 and strain Rd15 (phylotype I); CIP301 and CFBP2957 (phylotype IIA); NCPPB3987, UY031 and UW551 (phylotype IIB); and CMR15 (phylotype III). Interestingly, infection with phylotype IIA strains CIP301 and CFBP2957 resulted in root growth inhibition (Fig. 4a), root hair production (Fig. 4b) and cell death at the root tip (Fig. 4c), similar to what we observed with phylotype I and III strains. In contrast, phylotype IIB strains NCPPB3987, UY031 and UW551 did not cause growth inhibition, nor root hair production or cell death on infected roots. Thus, different *R. solanacearum* strains vary in their ability to cause the triple root phenotype. To determine whether these phenotypes correlated with pathogenicity, we performed root infection assays on Arabidopsis plants grown on soil and recorded the appearance of wilting symptoms over time (Fig. 4d). Infection of wild-type Col-0 plants with the strains that were unable to cause the triple root phenotype (NCPPB3987, UY031 and UW551) did not result in wilting, which indicates a direct correlation between absence of root phenotypes in vitro and absence of symptoms in plants grown in soil. On the contrary, from all *R. solanacearum* strains causing the triple root phenotype, only GMI1000, Rd15 and CMR15 resulted in plant wilting. As seen before for the *hrpG* and *hrpB* mutants, symptom scoring has limitations to evaluate slight *R. solanacearum* pathogenicity differences. Thus, we inoculated Arabidopsis plants with all studied bacterial strains and measured bacterial numbers in the aerial part 14 dpi. The results, shown in figure 4e, indicated that the two phylotype IIA strains (CIP301 and CFBP2957) that showed the triple phenotype but were not causing disease colonized the aerial part of the plants to higher numbers than the strains not causing the root responses. These results show that Arabidopsis root phenotypes partially correlate with the capacity of *R. solanacearum* to colonize Arabidopsis Col-0 plants: the strains that are not able to produce the triple root phenotype are non-virulent.

R. solanacearum-triggered root hair formation is mediated by plant auxins

In order to ascertain whether any of the phenotypes triggered by *R. solanacearum* infection were mediated by known plant defense regulators, we tested how different Arabidopsis mutants responded to the pathogen (Fig. S4). Our results showed that reactive oxygen species (ROS) produced by the membrane NADPH oxidases AtRbohD and AtRbohF were not required for root growth inhibition, root hair production or cell death in response to infection. Plants that were insensitive to jasmonic acid (*jai3-1*) or that could not synthetize it (*dde2*) or its conjugated form (*jar1-1*) showed root growth

inhibition, root hair production and cell death similar to the wild-type. Similarly, the *sid2* mutant, defective in salicylic acid biosynthesis, and the ethylene insensitive mutant *ein2*, responded with the same root morphologies as wild-type to *R. solanacearum* infection. On the contrary, the auxin insensitive mutants *tir1* and *tir1/afb2* showed growth inhibition (Fig. 5a) and root tip cell death (Fig. 5b) but were not able to produce root hairs in response to infection (Fig. 5c). This result indicates that root hair production triggered by *R. solanacearum* infection requires auxin signaling. To monitor potential changes in auxin levels during infection, we analyzed expression of the auxin signaling reporter *DR5rev::GFP* in roots of infected versus control plants. As shown in Fig. 5d, *R. solanacearum* inoculation induced a strong vascular GFP signal 48 hours post-infection, suggesting that infection may result in increased auxin signaling levels in the vascular cylinder.

R. solanacearum encodes a HrpG-regulated ethylene-forming enzyme (*efe*) gene (Valls *et al.*, 2006). To assess whether bacterial ethylene mediated root growth inhibition, we infected wild-type Arabidopsis with *R. solanacearum* GMI1000 wild-type strain or with the *efe* mutant. Fig. S5(a) show that infection with the mutant resulted in root growth inhibition, indicating that ethylene produced by the bacteria is not responsible for this phenotype. Bacterial ethylene was also not required for the root hair formation phenotype, because infection with the *efe* mutant did not affect root hair formation (Fig. S5b), as expected if HrpB –which does not activate the *efe* operon– controls this phenotype (figure 2b).

Absence of the triple root phenotype in Arabidopsis might reveal new sources of resistance to strain GMI1000

Next, we wanted to determine the degree of conservation of the correlation between absence of the triple phenotype and resistance to *R. solanaceraum*. For this, besides Col-0, we selected the accessions C24, Cvi-0, Ler-1, Bl-1, Rrs-7 among the 20 proposed as representatives of the maximum variability of Arabidopsis (Delker *et al.*, 2010). In addition, we included Nd-1, known to be resistant to *R. solanacearum* (Deslandes et al., 1998) and Tou-A1-74, which does not show the triple phenotype (see below). Despite the differences in root length among accessions, the majority of them displayed the triple root phenotype after inoculation with *R. solanacearum* (Fig. 6a, b, c). Only Rrs-7 and Tou-A1-74 did not show any of the three phenotypes in response to infection. To determine whether the presence/absence of the triple phenotype correlated to

susceptibility to *R. solanacearum* GMI1000, we performed a pathogenicity assay using these accessions (Fig. 6d). Interestingly, Rrs-7 –but not Tou-A1-74- was resistant to *R. solanacearum*, indicating that absence of the root phenotypes could be used to identify some sources of resistance to the pathogen. Resistance to *R. solanacearum* was not found in random accessions showing the triple root phenotype, which however did not correlate with susceptibility, since the resistant accessions Nd-1 (Deslandes *et al.*, 1998) and Bl-1 reacted with root growth inhibition, root hair production and cell death after infection (Fig. 6d).

Discussion

Plant host root phenotypes appear as early symptoms of colonization by *R. solanacearum*

The use of *in vitro* pathosystems to study the interactions between the vascular pathogen *R. solanacearum* and some of its plant hosts has emerged as a very powerful technique to understand the early stages of infection (Vasse *et al.*, 1995; Vasse *et al.*, 2000; Zolobowska & Van Gijsegem, 2006; Vailleau *et al.*, 2007; Turner *et al.*, 2009; Digonnet *et al.*, 2012). In this work, we have used *in vitro*-grown Arabidopsis as the model host to deepen our knowledge on the first steps of *R. solanacearum* root invasion. In vitro infection has several advantages: i) it reveals easily screenable root phenotypes associated with the infection that would remain hidden when using the soil-drench inoculation; ii) it facilitates microscopy studies to determine the penetration point and the infection itinerary through the root cell layers; iii) it is a useful tool to study the genetic determinants controlling both *R. solanacearum* virulence and host defense.

A very detailed microscopic analysis of the gnotobiotic Arabidopsis-*R. solanacearum* interaction has been recently published (Digonnet *et al.*, 2012). This study revealed the path followed by *R. solanacearum* through Arabidopsis roots, highlighting the sites of bacterial multiplication and the specific cell wall barriers degraded by the bacterium. Moving forward this knowledge, our data defines a set of root phenotypes associated to infection that can be correlated to bacterial aggressiveness and plant resistance and are genetically amenable both from the bacterial and the plant side.

In our system, infection of intact roots with a droplet of *R. solanacearum* resulted in root growth inhibition, root hair production and cell death. Root growth inhibition or

delayed elongation has been previously observed as a result of *R. solanacearum* infection when using gnotobiotic systems (Vasse *et al.*, 1995; Zolobowska & Van Gijsegem, 2006; Vailleau *et al.*, 2007; Turner *et al.*, 2009; Digonnet *et al.*, 2012). One could hypothesize that root growth inhibition is the direct cause of the massive cell death observed after infection in the root cortex of Arabidopsis (this work and (Digonnet *et al.*, 2012)) or other species (Vasse *et al.*, 1995; Turner *et al.*, 2009). However, this does not seem to be the case, since a *hrpB* mutant strain causes root growth inhibition in the absence of cell death. Considering this, root growth inhibition would rather reflect xylem colonization, which takes place both for wild-type *R. solanacearum* GMI1000 and the *hrpB* mutant. In agreement with this interpretation, the *hrpG* mutant, which has an extremely reduced capacity to invade the xylem (Fig. S3, (Vasse *et al.*, 1995; Vasse *et al.*, 2000)), does not cause root growth inhibition after infection. This further highlights the proposed role of HrpG as a central regulator controlling still-unknown activities essential for the bacterium to reach and multiply in the plant xylem (Vasse *et al.*, 2000; Valls *et al.*, 2006). These activities are likely encoded in genes regulated by HrpG independently of HrpB, as the latter is able to colonize the xylem. Amongst the 184 genes specifically regulated by HrpG, an obvious candidate responsible for the root growth inhibition is the gene controlling bacterial production of the phytohormone ethylene. However, we found that bacterial mutant defective in this gene still inhibited root growth (figure S5a), indicating that xylem colonization and subsequent root inhibition is controlled by other still-undefined HrpG-regulated genes.

Auxin signaling alterations caused by *R. solanacearum* infection likely trigger root structure rearrangements, resulting in root hair formation

Our plant mutant analysis showed that neither of the defense regulators salicylic acid, jasmonic acid, ethylene or NADPH-produced ROS were required for any of the root phenotypes observed after *R. solanacearum* GMI1000 infection. On the contrary, we showed that auxin signaling was clearly required for infection-triggered root hair formation. This is not surprising, since auxin is one of the main orchestrators of root hair formation (Lee & Cho, 2013; Grierson *et al.*, 2014) and can promote this process (Pitts *et al.*, 1998). Root hairs are outgrowths of epidermal cells that contribute to nutrient and water absorption (Grierson *et al.*, 2014), but they also participate in plant-microbe interactions. For instance, root hairs are the entry point of both mutualistic

rhizobacteria (Rodriguez-Navarro *et al.*, 2007) and pathogenic bacteria such as *Plasmodiophora brassicaceae*, the causing agent of the clubroot disease (Kageyama & Asano, 2009). Interestingly, auxin signaling was proposed to promote cell wall remodeling to allow root hair growth (Breakspear *et al.*, 2014) and it has been shown to be a key component of both pathogenic and mutualistic root hair infections (Jahn *et al.*, 2013; Laplaze *et al.*, 2015).

During *R. solanacearum*-Arabidopsis interactions, auxin signaling may have additional important roles beyond its involvement in root hair formation. *R. solanacearum* inoculation resulted in an induction of *DR5rev::GFP* expression in the root vascular cylinder at early stages of infection, indicative of increased auxin signaling levels. Furthermore, plant infection results in increased expression of several auxin-related genes (Zuluaga *et al.*, 2015). On a hypothetic scenario, *R. solanacearum* could directly and specifically –for example, via a T3SS effector– manipulate the host auxin signaling pathway(s) to its own benefit. There are many examples of effector-mediated manipulation of the host auxin pathway, extensively reviewed by Kazan & Lyons (2014). In most cases the pathogen uses its type III effector arsenal to specifically increase auxin levels in the host by targeting auxin biosynthesis, signaling or transport. Elevated auxin levels are beneficial for many pathogens, towards which auxin promotes susceptibility. This is the case of *Pseudomonas syringae*, *Xanthomonas oryzae* and *Magnaporte oryzae*, among others. In rice, elevated susceptibility has been linked to auxin-induced loosening of the protective cell wall, which would facilitate pathogen colonization. Other pathogens increase the host susceptibility by secreting auxin into the host, which in turn induces auxin production inside the host's cells and promotes susceptibility (Fu *et al.*, 2011). Our data points towards a potential link between increased auxin levels as a result of invasion, although further work needs to be done to determine whether this is directly correlated with an increase in susceptibility. In this context, it also remains to be clarified whether auxin-mediated root hair formation during infection facilitates *R. solanacearum* invasion or it is a mere consequence of elevated auxin levels in certain root cells. Also, it is not known whether root hairs may constitute favorite entry points for the bacteria.

Absence of the triple root phenotype to screen for *R. solanacearum* virulence factors or resistance in Arabidopsis

When analyzing different *R. solanacearum* strains, the absence of the root phenotypes is directly linked to the inability of the bacterium to cause symptoms. Thus, strains not capable to induce the triple root phenotype show low pathogenicity on Arabidopsis, as it is the case of NCPPB3987, UY031 and UW551. Presence of the phenotype is not always correlated with increased aggressiveness of a particular strain. CIP301 and CFBP2957 are not pathogenic on Arabidopsis Col-0 plants despite causing the triple root phenotype. Gene-for-gene interactions may mask these root phenotypic features and block *R. solanacearum* before it starts causing wilt. This may indicate that the Col-0 accession possesses resistance proteins that recognize effectors secreted by the two phylotype IIA strains or that phylotype IIA strains lack one or several virulence factors required to establish disease on Arabidopsis or repress some plant defenses. Similarly, the *hrpG* mutant, which has an extremely reduced capacity to invade the xylem, does not cause root inhibition (see above).

Our data show that the lack of the triple root phenotype can be linked to resistance to *R. solanacearum*. This is the case of Arabidopsis accession Rrs-7, that appears completely resistant to *R. solanacearum* GMI1000 and does not display any of described root phenotypes. Resistance to *R. solanacearum* is very rare amongst Arabidopsis accessions. The clear enrichment of resistant accessions amongst those lacking the capacity to cause the triple phenotype indicates that the root phenotypes described here can be used to screen plant varieties in search for resistance. The fact that other resistant accessions present the phenotypes may indicate that they possess alternative forms of resistance or that other factors, including gene-for-gene interactions, override the observed phenotypes. This could be the case of the resistant accession Nd-1, which is able to detect *R. solanacearum* GMI1000 infection through recognition of the effector PopP2 by the resistance protein RRS1-R (Deslandes *et al.*, 2003). This system could thus be used to differentiate ecotypes with resistances due to a gene-for-gene recognition (Nd-1 resistance associated to the presence of the triple response) compared to other resistance mechanisms (Rrs-7 resistance associated to absence of the triple root response). Along this line, the Arabidopsis Bl-1, which also does not wilt but shows clear infection indicated by the appearance of the root phenotypes, may also recognize *R. solanacearum* through an alternative effector–resistance protein pair and stop invasion.

Taken together, our results on both the bacterial and the plant side favor the notion that absence of the root phenotypes is indicative of ineffective colonization that may reflect

novel forms of resistance. Thus, the absence of the root phenotypes described here could help in the search for plant varieties with higher resistance to the devastating bacterial wilt disease.

Materials and Methods

Biological material

Arabidopsis thaliana ecotypes Bl-1, C24, Col-0, Cvi-0, Ler-1, Nd-1, Rrs-7 (Delker *et al.*, 2010, Clark *et al.*, 2007), Tou-A1-74 (Horton *et al.*, 2012), and the Col-0 mutants: *sid2-2* (Tsuda *et al.*, 2009), *dde2-2* (Tsuda *et al.*, 2009), *ein2-1* (Tsuda *et al.*, 2009), *tir1-1* (Dharmasiri *et al.*, 2005), *tir1-1/afb2-3* (Parry *et al.*, 2009), *jar1-1* (Staswick & Tiryaki, 2004), *jai3-1* (Chini *et al.*, 2007), *atrbohD* and *atrbohF* (Torres *et al.*, 2002) were used. The Col-0 transgenic line *DR5rev::GFP* (Friml *et al.*, 2003) was used to monitor auxin signaling.

All *R. solanacearum* strains used are described in Supplementary Table1. Bacteria were grown at 28°C in solid or liquid rich B medium (1% Bactopeptone , 0.1% Yeast extract and 0.1% Casamino acids -all from Becton, Dickinson and Co., Franklin Lakes, NJ, USA) adding the appropriate antibiotics, as described in (Monteiro *et al.*, 2012).

In vitro inoculation assay

Seeds were sterilized with a solution containing 30% bleach and 0.02% Triton-X 100 for 10 min, washed five times with Milli-Q water and sown (20 seeds/plate) on MS-plates containing vitamins (Duchefa Biochemie B.V., Haarlem, the Nederlands) and 0.8% Agar (Becton, Dickinson and Co., Franklin Lakes, NJ, USA). Sown plates were stratifiedat 4°C in the dark for two days. Then plates were transferred to chambers and grown for 6-7 days under constant conditions of 21-22°C, 60% humidity and a 16h light/8h dark photoperiod.

For inoculation, *R. solanacearum* was collected by centrifugation (4000 rpm, 5 min) from overnight liquid cultures, resuspended with water and adjusted to a final OD_{600} of 0.01. Six to seven-day-old Arabidopsis seedlings grown on plates as detailed above were inoculated with 5 µL of the bacterial solution, which was applied 1cm above the root tip, as described previously (Digonnet *et al.*, 2012). Plates with the infected seedlings were sealed with micropore tape (3M Deutschland GmbH, Neuss, Germany)

and transferred to a controlled growth chamber at 25°C, 60% humidity and a 12h light/12h dark photoperiod. Root length of infected seedlings was recorded over time. For root hair evaluation, pictures were taken 6 days post inoculation (dpi) with an Olympus DP71 stereomicroscope (Olympus, Center Valley, PA, USA) at 11.5x. To analyze cell death, roots from seedlings grown on plates were collected 6 dpi and immediately stained by carefully submerging them into a solution containing 0.05% w/v of Evans blue (Sigma-Aldrich, Buchs, Switzerland) for 30 min at room temperature. Roots were then washed twice with distilled water and photographed under a 20× lens with a Nomarski Axiophot DP70 microscope (Zeiss, Oberkochen, Germany). For propidium iodide staining, roots of infected seedlings were soaked into 1µg/ml staining solution (Sigma-Aldrich, Buchs, Switzerland), and immediately photographed with a 20x magnification on an Olympus FV1000 (Olympus, Center Valley, PA, USA) or a Leica SP5 (Wetzlar, Germany) confocal microscope.

Pathogenicity assays

R. solanacearum pathogenicity tests were carried out using the soil-drench method (Monteiro *et al.*, 2012). Briefly, Arabidopsis was grown for 4-to-5 weeks on Jiffy pots (Jiffy Group, Lorain, OH, USA) in a controlled chamber at 22°C, 60% humidity and a 8h light/16h dark photoperiod. Jiffys were cut at 1/3 from the bottom and immediately submerged for 30 min into a solution of overnight-grown *R. solanacearum* adjusted to OD_{600}=0.1 with distilled water (35 ml of bacterial solution per plant). Then inoculated plants were transferred to trays containing a thin layer of soil drenched with the same *R. solanacearum* solution and kept in a chamber at 28°C, 60% humidity and 12h light/12h dark. Plant wilting symptoms were recorded every day and expressed according to a disease index scale (0: no wilting, 1: 25% wilted leaves, 2: 50%, 3: 75%, 4: death). At least 30 plants were used in each assay, performed at least in three replicate experiments.

R. solanacearum vessel colonization was tested in Arabidopsis plants inoculated with a lower inoculum (OD_{600}= 0.01). To quantify bacterial colonization, the plant aerial parts were cut 14 days after inoculation and homogenized. Dilutions of the homogenate plant material were plated on rich B medium supplemented with the appropriate antibiotics and the bacterial content measured as colony formation units (cfu) per gram of fresh plant tissue. At least 20 plants were inoculated per *R. solanacearum* strain and the experiment was repeated three times.

Acknowledgements

We are grateful to M. Estelle (University of California San Diego) for the *tir1* and *tir1/afb2* seeds; to K. Tsuda (Max Planck Institute from plant breeding research) for the *sid2*, *ein2* and *dde2* seeds; to R. Solano (Spanish National Center for Biotechnolgy, CNB) for the *jai3-1* and *jar1-1* seeds; and to M. Quint (Leibniz institute of Plant Biochemistry), for the Arabidopsis accessions Bl-1, C24, Cvi-0, Ler-1, Nd-1 and RRS-7. We would like to thank M.A. Moreno-Risueño for helpful comments and critically reading the manuscript. We also thank S. Poussier, I. Robène, E. Wicker, S. Genin, CP. Cheng, P Hanson and P. Prior for providing *R. solanacearum* strains and for their advice in the choice of relevant ones. This work was funded by MINECO projects AGL2013-46898-R and AGL2016-78002-R to N.S.C. and M.V. and RyC 2014-1658 to N.S.C. and EU-Marie Curie Actions (PCDMC-321738 and PIIF-331392) and BP_B 00030 from the Catalan Government to N.S.C. We also want to acknowledge the support of the COST Action SUSTAIN (FA1208), the "Severo Ochoa Programme for Centres of Excellence in R&D" 2016-2019 (SEV-2015-0533) from the MINECO and by the CERCA Programme / Generalitat de Catalunya.

References

Boucher CA, Barberis PA, Trigalet AP, Demery DA. 1985. Transposon mutagenesis of *Pseudomonas solanacearum*: isolation of Tn5-induced avirulent mutants. *J.Gen.Microbiol.* 131: 2449-2457.

Breakspear A, Liu C, Roy S, Stacey N, Rogers C, Trick M, Morieri G, Mysore KS, Wen J, Oldroyd GE, et al. 2014. The root hair "infectome" of Medicago truncatula uncovers changes in cell cycle genes and reveals a requirement for Auxin signaling in rhizobial infection. *Plant Cell* 26(12): 4680-4701.

Brito B, Aldon D, Barberis P, Boucher C, Genin S. 2002. A signal transfer system through three compartments transduces the plant cell contact-dependent signal controlling R. solanacearum hrp genes. *Mol Plant Microbe Interact* 15(2): 109-119.

492 Clark RM, Schweikert G, et al. 2007. Common Sequence Polymorphisms Shaping
493 Genetic Diversity in Arabidopsis thaliana. *Science* 317(5836): 338-342.
494 Cruz AP, Ferreira V, Pianzzola MJ, Siri MI, Coll NS, Valls M. 2014. A novel, sensitive
495 method to evaluate potato germplasm for bacterial wilt resistance using a
496 luminescent Ralstonia solanacearum reporter strain. *Mol Plant Microbe Interact*
497 27(3): 277-285.
498 Curtis MJ, Hays JB. 2007. Tolerance of dividing cells to replication stress in UVB-
499 irradiated Arabidopsis roots: requirements for DNA translesion polymerases eta
500 and zeta. *DNA Repair (Amst)* 6(9): 1341-1358.
501 Chini A, Fonseca S, Fernandez G, Adie B, Chico JM, Lorenzo O, Garcia-Casado G,
502 Lopez-Vidriero I, Lozano FM, Ponce MR, et al. 2007. The JAZ family of
503 repressors is the missing link in jasmonate signalling. *Nature* 448(7154): 666-
504 671.
505 Delker C, Poschl Y, Raschke A, Ullrich K, Ettingshausen S, Hauptmann V, Grosse I,
506 Quint M. 2010. Natural variation of transcriptional auxin response networks in
507 Arabidopsis thaliana. *Plant Cell* 22(7): 2184-2200.
508 Deslandes L, Olivier J, Peeters N, Feng DX, Khounlotham M, Boucher C, Somssich I,
509 Genin S, Marco Y. 2003. Physical interaction between RRS1-R, a protein
510 conferring resistance to bacterial wilt, and PopP2, a type III effector targeted to
511 the plant nucleus. *Proc Natl Acad Sci U S A* 100(13): 8024-8029.
512 Deslandes L, Pileur F, Liaubet L, Camut S, Can C, Williams K, Holub E, Beynon J,
513 Arlat M, Marco Y. 1998. Genetic characterization of RRS1, a recessive locus in
514 Arabidopsis thaliana that confers resistance to the bacterial soilborne pathogen
515 Ralstonia solanacearum. *Mol Plant Microbe Interact* 11(7): 659-667.
516 Dharmasiri N, Dharmasiri S, Estelle M. 2005. The F-box protein TIR1 is an auxin
517 receptor. *Nature* 435(7041): 441-445.
518 Digonnet C, Martinez Y, Denance N, Chasseray M, Dabos P, Ranocha P, Marco Y,
519 Jauneau A, Goffner D. 2012. Deciphering the route of Ralstonia solanacearum
520 colonization in Arabidopsis thaliana roots during a compatible interaction: focus
521 at the plant cell wall. *Planta* 236(5): 1419-1431.
522 Friml J, Vieten A, Sauer M, Weijers D, Schwarz H, Hamann T, Offringa R, Jurgens G.
523 2003. Efflux-dependent auxin gradients establish the apical-basal axis of
524 Arabidopsis. *Nature* 426(6963): 147-153.

525 Fu J, Liu H, Li Y, Yu H, Li X, Xiao J, Wang S. 2011. Manipulating broad-spectrum
526 disease resistance by suppressing pathogen-induced auxin accumulation in rice.
527 *Plant Physiol* 155(1): 589-602.
528 Gaff DF, Okong'O-gola O. 1971. The use of non-permeating pigments for testing the
529 survival of cells. *J Exp Bot* 22: 757-758.
530 Galan JE, Collmer A. 1999. Type III secretion machines: Bacterial devices for protein
531 delivery into host cells. *Science* 284(5418): 1322-1328.
532 Genin S. 2010. Molecular traits controlling host range and adaptation to plants in
533 Ralstonia solanacearum. *New Phytol* 187(4): 920-928.
534 Genin S, Denny TP. 2012. Pathogenomics of the Ralstonia solanacearum species
535 complex. *Annu Rev Phytopathol* 50: 67-89.
536 Grierson C, Nielsen E, Ketelaarc T, Schiefelbein J. 2014. Root hairs. *Arabidopsis Book*
537 12: e0172.
538 Hayward AC. 1991. Biology and epidemiology of bacterial wilt caused by
539 pseudomonas solanacearum. *Annu Rev Phytopathol* 29: 65-87.
540 Hanemian M., Zhou B., Deslandes L., Marco Y., Trémousaygue D. 2013. Hrp mutant
541 bacteria as biocontrol agents: Toward a sustainable approach in the fight against
542 plant pathogenic bacteria. *Plant Signaling & Behavior*, 8(10), e25678.
543 Horton MW, Hancock AM, Huang YS, Toomajian C, Atwell S, Auton A, Muliyati NW,
544 Platt A, Sperone FG, Vilhjálmsson BJ, Nordborg M, Borevitz JO, Bergelson J.
545 2012. Genome-wide patterns of genetic variation in worldwide *Arabidopsis*
546 *thaliana* accessions from the RegMap panel. *Nat Genet*. 2012 44(2):212-216.
547 Hueck CJ. 1998. Type III protein secretion systems in bacterial pathogens of animals
548 and plants. *Microbiol Mol Biol Rev* 62(2): 379-433.
549 Jahn L, Mucha S, Bergmann S, Horn C, Staswick P, Steffens B, Siemens J, Ludwig-
550 Müller J. 2013. The Clubroot Pathogen (Plasmodiophora brassicae) Influences
551 Auxin Signaling to Regulate Auxin Homeostasis in Arabidopsis. *Plants* 2(4):
552 726-749.
553 Kageyama K, Asano T. 2009. Life Cycle of Plasmodiophora brassicae. *Journal of Plant*
554 *Growth Regulation* 28(3): 203-211.
555 Kazan K, Lyons R. 2014. Intervention of Phytohormone Pathways by Pathogen
556 Effectors. *Plant Cell* 26(6): 2285-2309.
557 Laplaze L, Lucas M, Champion A. 2015. Rhizobial root hair infection requires auxin
558 signaling. *Trends Plant Sci* 20(6): 332-334.

559 Lee RD, Cho HT. 2013. Auxin, the organizer of the hormonal/environmental signals for
560 root hair growth. *Front Plant Sci* 4: 448.
561 Lindgren PB, Peet RC, Panopoulos NJ. 1986. Gene cluster of Pseudomonas syringae
562 pv. phaseolicola controls pathogenicity of bean plants and hypersensitivity of
563 nonhost plants. *Journal of Bacteriology*, *168*(2), 512–522.
564 Mansfield J, Genin S, Magori S, Citovsky V, Sriariyanum M, Ronald P, Dow M,
565 Verdier V, Beer SV, Machado MA, et al. 2012. Top 10 plant pathogenic bacteria
566 in molecular plant pathology. *Mol Plant Pathol* 13(6): 614-629.
567 Monteiro F, Sole M, van Dijk I, Valls M. 2012. A chromosomal insertion toolbox for
568 promoter probing, mutant complementation, and pathogenicity studies in
569 Ralstonia solanacearum. *Mol Plant Microbe Interact* 25(4): 557-568.
570 Parry G, Calderon-Villalobos LI, Prigge M, Peret B, Dharmasiri S, Itoh H, Lechner E,
571 Gray WM, Bennett M, Estelle M. 2009. Complex regulation of the TIR1/AFB
572 family of auxin receptors. *Proc Natl Acad Sci U S A* 106(52): 22540-22545.
573 Pitts RJ, Cernac A, Estelle M. 1998. Auxin and ethylene promote root hair elongation in
574 Arabidopsis. *Plant J* 16(5): 553-560.
575 Rodriguez-Navarro DN, Dardanelli MS, Ruiz-Sainz JE. 2007. Attachment of bacteria to
576 the roots of higher plants. *FEMS Microbiol Lett* 272(2): 127-136.
577 Saile E, McGarvey JA, Schell MA, Denny TP. 1997. Role of Extracellular
578 Polysaccharide and Endoglucanase in Root Invasion and Colonization of
579 Tomato Plants by Ralstonia solanacearum. *Phytopathology* 87(12): 1264-1271.
580 Staswick PE, Tiryaki I. 2004. The oxylipin signal jasmonic acid is activated by an
581 enzyme that conjugates it to isoleucine in Arabidopsis. *Plant Cell* 16(8): 2117-
582 2127.
583 Torres MA, Dangl JL, Jones JD. 2002. Arabidopsis gp91phox homologues AtrbohD
584 and AtrbohF are required for accumulation of reactive oxygen intermediates in
585 the plant defense response. *Proc Natl Acad Sci U S A* 99(1): 517-522.
586 Tsuda K, Sato M, Stoddard T, Glazebrook J, Katagiri F. 2009. Network properties of
587 robust immunity in plants. *PLoS Genet* 5(12): e1000772.
588 Turner M, Jauneau A, Genin S, Tavella MJ, Vailleau F, Gentzbittel L, Jardinaud MF.
589 2009. Dissection of bacterial Wilt on Medicago truncatula revealed two type III
590 secretion system effectors acting on root infection process and disease
591 development. *Plant Physiol* 150(4): 1713-1722.

592 Vailleau F, Sartorel E, Jardinaud MF, Chardon F, Genin S, Huguet T, Gentzbittel L,
593 Petitprez M. 2007. Characterization of the interaction between the bacterial wilt
594 pathogen Ralstonia solanacearum and the model legume plant Medicago
595 truncatula. *Mol Plant Microbe Interact* 20(2): 159-167.
596 Valls M, Genin S, Boucher C. 2006. Integrated regulation of the type III secretion
597 system and other virulence determinants in Ralstonia solanacearum. *PLoS*
598 *Pathog* 2(8): e82.
599 Vasse J, Frey P, Trigalet A. 1995. Microscopic studies of intercellular infection and
600 protoxylem invasion of tomato roots by Pseudomonas solanacearum. *Molecular*
601 *Plant-Microbe Interactions* 8(2): 241-251.
602 Vasse J, Genin S, Frey P, Boucher C, Brito B. 2000. The hrpB and hrpG regulatory
603 genes of Ralstonia solanacearum are required for different stages of the tomato
604 root infection process. *Mol Plant Microbe Interact* 13(3): 259-267.
605 Zolobowska L, Van Gijsegem F. 2006. Induction of lateral root structure formation on
606 petunia roots: A novel effect of GMI1000 Ralstonia solanacearum infection
607 impaired in Hrp mutants. *Mol Plant Microbe Interact* 19(6): 597-606.
608 Zuluaga AP, Sole M, Lu H, Gongora-Castillo E, Vaillancourt B, Coll N, Buell CR,
609 Valls M. 2015. Transcriptome responses to Ralstonia solanacearum infection in
610 the roots of the wild potato Solanum commersonii. *BMC Genomics* 16: 246.

611

612 **Figure Legends**

613

614 **Figure 1. Root phenotypes caused by *R. solanacearum* GMI1000 (GMI1000) in**
615 **vitro infection.** 6-day-old Col-0 seedlings were inoculated with 5µL of a GMI1000
616 solution or with water as a control. (A) GMI1000 inhibition of root growth. Left panel:
617 stereoscope images of the plantlets under white light at 6 days post inoculation (dpi).
618 Right panel: root length at different times after infection. (B) Root hair formation on the
619 root tip caused by GMI1000 infection. Root tip pictures obtained as before at 6 dpi. (C)
620 Observation of cell death at root tips visualized by Evans blue staining. Representative
621 Nomarski microscope pictures of stained roots obtained 6 dpi.10-15 plants were used in
622 3 independent experiments.

623

Figure 2. HrpG is required for all the phenotypes caused by GMI1000 while HrpB is only essential for cell death and root hair formation. 6-day-old Col-0 seedlings were inoculated with water (control) or with the following strains: GMI1000 wild type (WT), *ΔhrpG* (whole gene deletion), *hrpG* (Tn5 transposon insertion), *ΔhrpG*(*hrpG*), *hrpB* (Tn5 transposon insertion) and *hrpBΩ* (Ω cassette insertion). (A) Mutations on HrpG but not HrpB abolish growth inhibition. Left panel: picture taken at 9 dpi. Right panel: root growth measurements at 9 dpi. (B) Both *hrpG* and *hrpB* mutations abolish root hair formation. Pictures were taken at 6 dpi. (C) Neither *hrpG* nor *hrpB* mutant cause root tip cell death. Pictures of infected seedlings at 6 dpi stained with Evans blue as in figure 1C. Each experiment was repeated at least 3 times using 5-10 plants.

Figure 3. Detection of plant signals is essential for GMI1000 to cause root growth inhibition. Six-day-old Col-0 seedlings were inoculated with GMI1000 (WT), its derivative strains disrupted for components of the *hrp* signaling cascade or treated with water. (A) Root growth was measured at 9 dpi and (B) pictures were taken at 9 dpi. Letters above bars indicate statistical significance; bars not sharing letters represent significant mean differences by one-way ANOVA ($p < 0.05$, $\alpha = 0.05$) with post-hoc Scheffé ($\alpha = 0.05$). 5-7 plants were used in 3 independent experiments.

Figure 4. The ability to cause root growth inhibition, root hair formation and cell death varies across different *R. solanacearum* strains. Six-day-old Col-0 seedlings were inoculated with the indicated *R. solanacearum* wild-type strains or water. (A) Root growth after infection at 6 dpi. (B) Pathogenicity assay. (C) Bacterial multiplication in planta measured 14 days after inoculation. For graphs (A-C) letters indicate statistical significance; values not sharing letters represent significant mean differences by one-way ANOVA ($p < 0.05$, $\alpha = 0.05$) with post-hoc Scheffé ($\alpha = 0.05$). In (B), the statistical test was applied separately for each dpi. (D) Root hair formation at 6 dpi. (E) Roots from infected seedlings at 6 dpi stained with Evans blue. Each experiment was repeated at least 3 times using 10-15 plants.

Figure 5. Auxin signaling is required for *R. solanacearum*-triggered root hair formation in Arabidopsis, but not for root growth inhibition and cell death. Six-day-old Col-0, *tir1* and *tir1/afb2* seedlings were inoculated with *R. solanacearum* GMI1000 or water and: (A) root growth was measured 6 dpi; (B) root hair formation

was evaluated at 6 dpi; and (C) roots from infected seedlings at 6 dpi were stained with Evans blue. (D) Expression of the auxin signaling marker *DR5* was analyzed under the confocal microscope in roots of transgenic Col-0 *DR5rev::GFP* plants infected with *R. solanacearum* GMI1000 or water at 24 and 48 hours after inoculation (hpi). Representative pictures of both the meristem area and maturation zone are shown. 6-10 plants were used in 3 different experimental replicates.

Figure 6. The absence of the triple phenotype caused by *R. solanacearum* in Arabidopsis is indicative of resistance. Six-day-old Arabidopsis seedlings from ecotypes C24, Col-0, Cvi-0, Ler-1, Nd-1, Rrs-7, Bl-1 and Tou-A1-74 were inoculated with *R. solanacearum* GMI1000 or water and at 6 dpi root growth was measured (A), root hair was visualized (B) and cell death was observed after Evans blue staining (C). (D) Five-week old plants grown in Jiffy pots were inoculated with GMI1000. Disease Index indicates the symptoms measured in a 1 to 4 scale as described in methods. Letters indicate statistical significance; values not sharing letters represent significant mean differences by one-way ANOVA ($p < 0.05$, $\alpha = 0.05$) with post-hoc Scheffé ($\alpha = 0.05$). The statistical test was applied separately for each dpi. 7-13 plants were used in each of 3 independent experiments.

Supplementary Figure Legends

Supplementary Table 1 *R. solanacearum* strains were used in this study.

Figure S1. The root site of infection does not have effect on growth inhibition caused by *R. solanacearum* GMI1000. Six-day-old Col-0 seedlings were inoculated with GMI1000 or water. Left panel: Picture of a 6-day-old seedling before infection, with yellow arrows pointing at the selected positions for R. solanacearum infection. Right panel: root growth inhibition occurs independently of the site of infection. 5-8 plants were used in at least 3 different experiments

Figure S2. *R. solanacearum*-triggered cell death at the root tip visualized using propidium iodide staining. Photographs were taken using confocal microscopy at 6 dpi.

Figure S3. *R. solanacearum* GMI1000 Wt, *hrpB* and *hrpG* mutants show different plant colonization capacity compared to Wt. Four-week old plants grown in Jiffy pots were inoculated with the following strains: GMI1000 Wt, hrpB (Tn5 transposon insertion) and hrpG (Tn5 transposon insertion) at OD600 of 0.01 (107 cfu/mL). At 14 dpi

692 bacterial load was calculated; three different experiments are plotted, with a total of 10
693 plants for the Wt control, 20 plants for hrpB and 20 plants for hrpG. Letters indicate
694 statistical significance; values not sharing letters represent significant mean differences
695 by post-hoc Tukey´s ($p < 0.05$)
696 **Figure S4.** The plant defense regulators jasmonic acid, ethylene, salicylic acid and
697 reactive oxygen species are not essential for the triple phenotype caused by R.
698 solanacearum GMI1000 infection. Six-day-old mutant dde2, jai3-1, jar1-1, sid2, ein2,
699 atrbohD, atrbohF and wild type Col-0 seedlings were inoculated with GMI1000 or
700 water. (A) Root growth was measured at 6 dpi. (B) Root hair formation was
701 photographed at 6 dpi. (C) Cell death was observed by Evans blue staining at 6 dpi
702 using Nomarski microscopy. Around 6-10 plants were used in at least 3 different
703 experiments.
704 **Figure S5**. Ethylene produced by GMI1000 is not required for root growth inhibition,
705 root hair formation nor cell death. (A) Disruption of the ethylene forming enzyme gene
706 efe does not abolish root growth inhibition and (B) it does not affect root hair formation
707 nor cell death caused by GMI1000. 6-day-old Col-0 seedlings were inoculated with
708 GMI1000 or water. Infected seedlings were photographed at 9 dpi and root growth was
709 measured at 9 dpi. Root hair formation and cell death was stained as in fig. 1 and
710 photographed at 6 dpi. 10-14 plants were used in 3 independent experiments
711
712

A

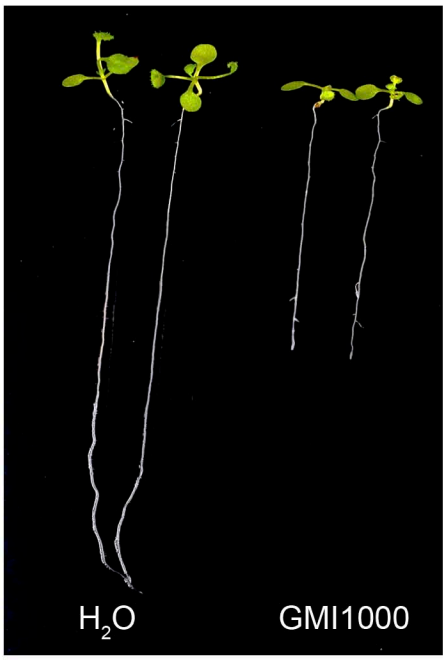
H2O
GMI1000

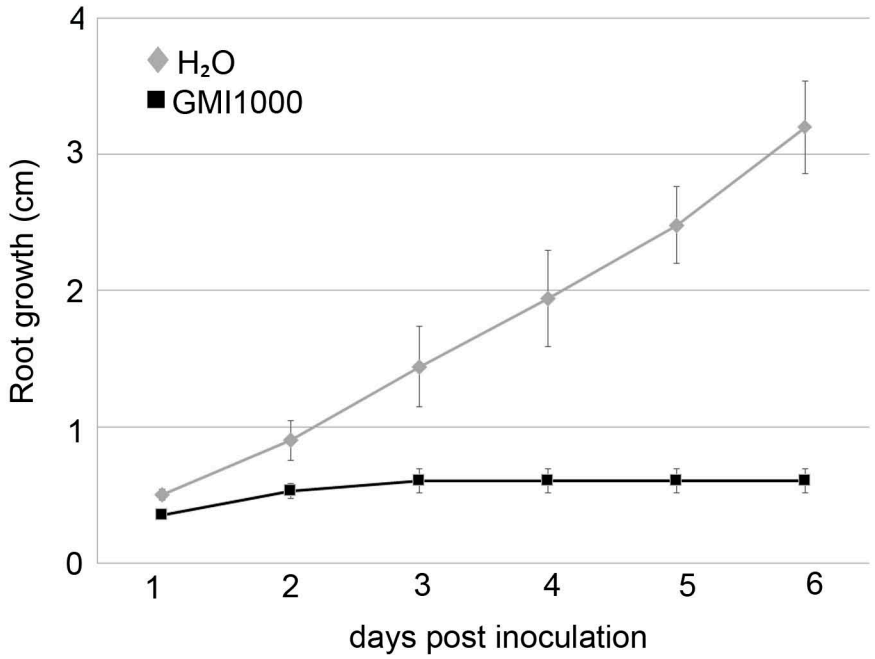
H2O
GMI1000
Root growth (cm)
0
1
2
3
4
1
2
3
4
5
6
days post inoculation

B


H2O
GMI1000

C

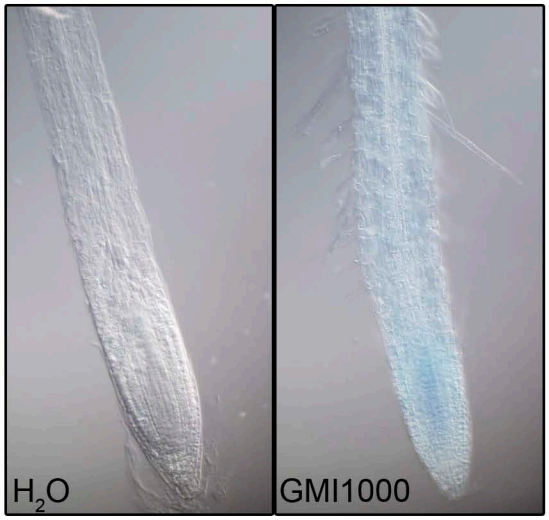
H2O
GMI1000

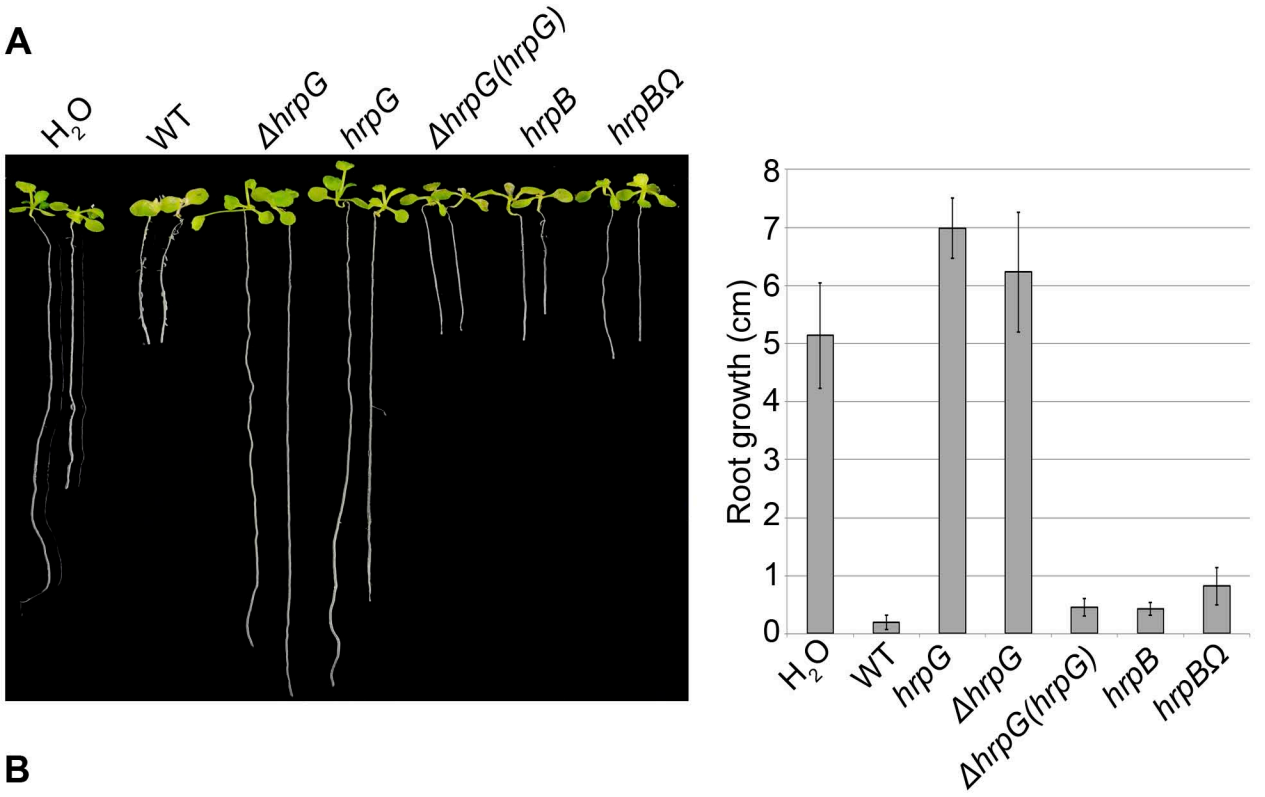
A
H2O
WT
ΔhrpG
hrpG
ΔhrpG(hrpG)
hrpB
hrpBΩ
Root growth (cm)
0
1
2
3
4
5
6
7
8
H2O
WT
hrpG
ΔhrpG
ΔhrpG(hrpG)
hrpB
hrpBΩ

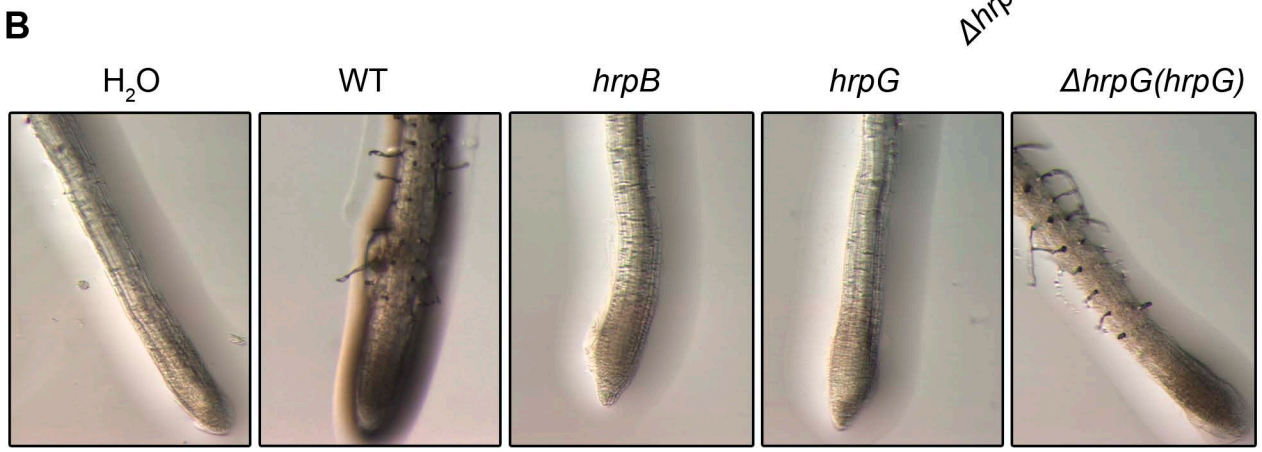
B
H2O
WT
hrpB
hrpG
ΔhrpG(hrpG)

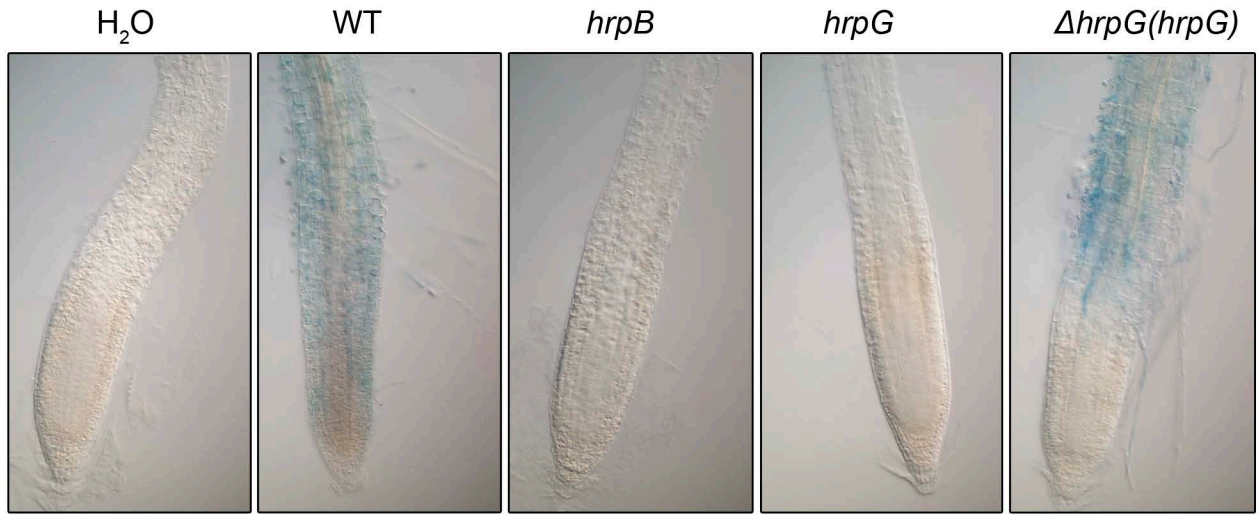
C
H2O
WT
hrpB
hrpG
ΔhrpG(hrpG)

A

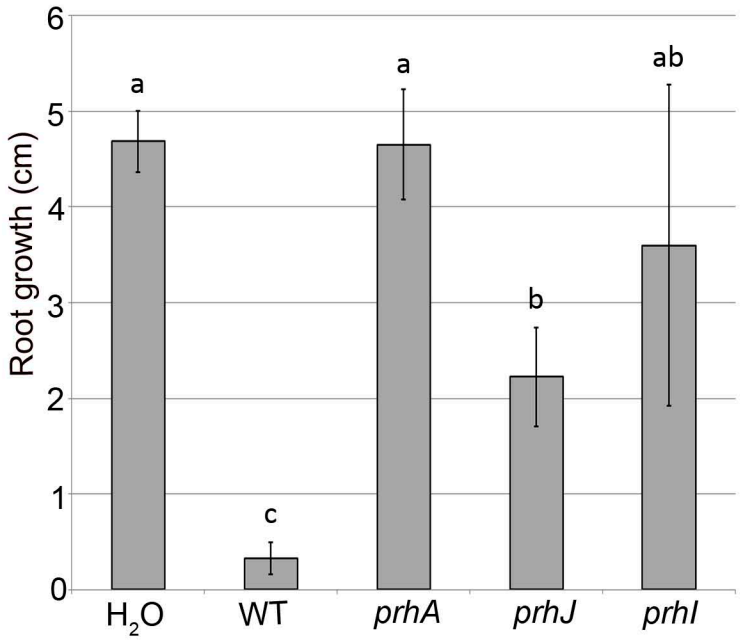
Root growth (cm)
0
1
2
3
4
5
6
a
c
a
b
ab
H2O
WT
prhA
prhJ
prhI

B

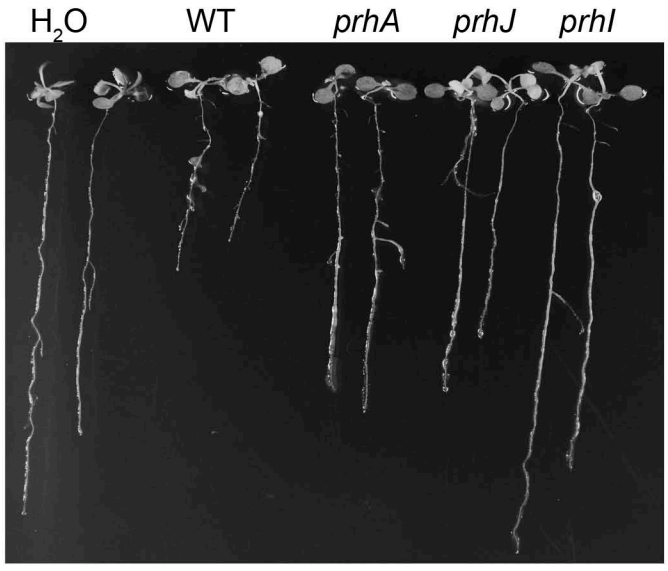
H2O
WT
prhA
prhJ
prhI

A

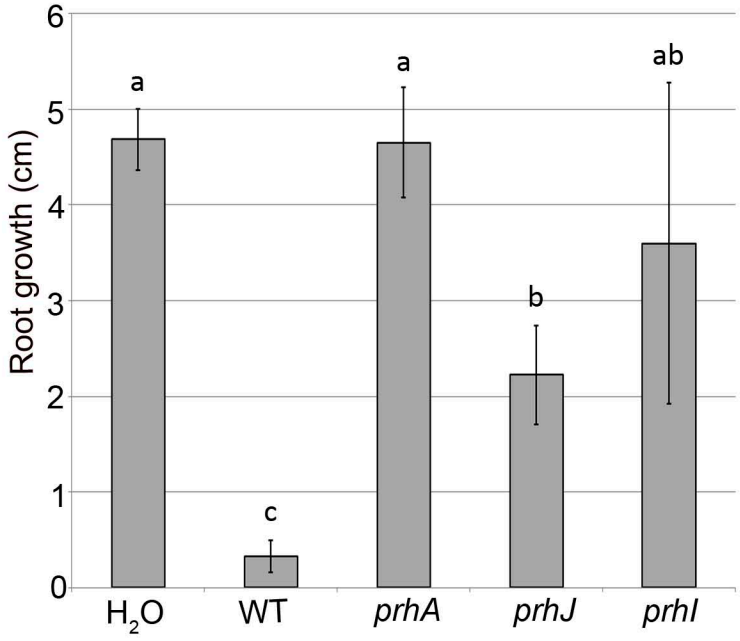
Root growth (cm)
0
1
2
3
4
5
6
a
c
a
b
ab
H2O
WT
prhA
prhJ
prhI

B

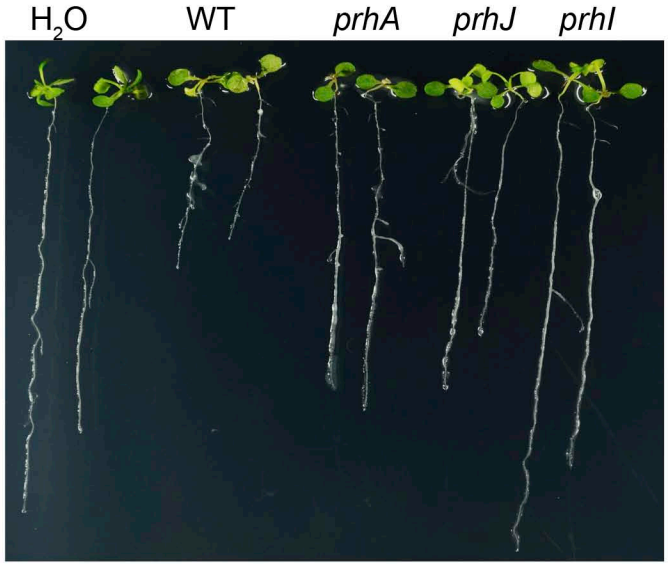
H2O
WT
prhA
prhJ
prhI

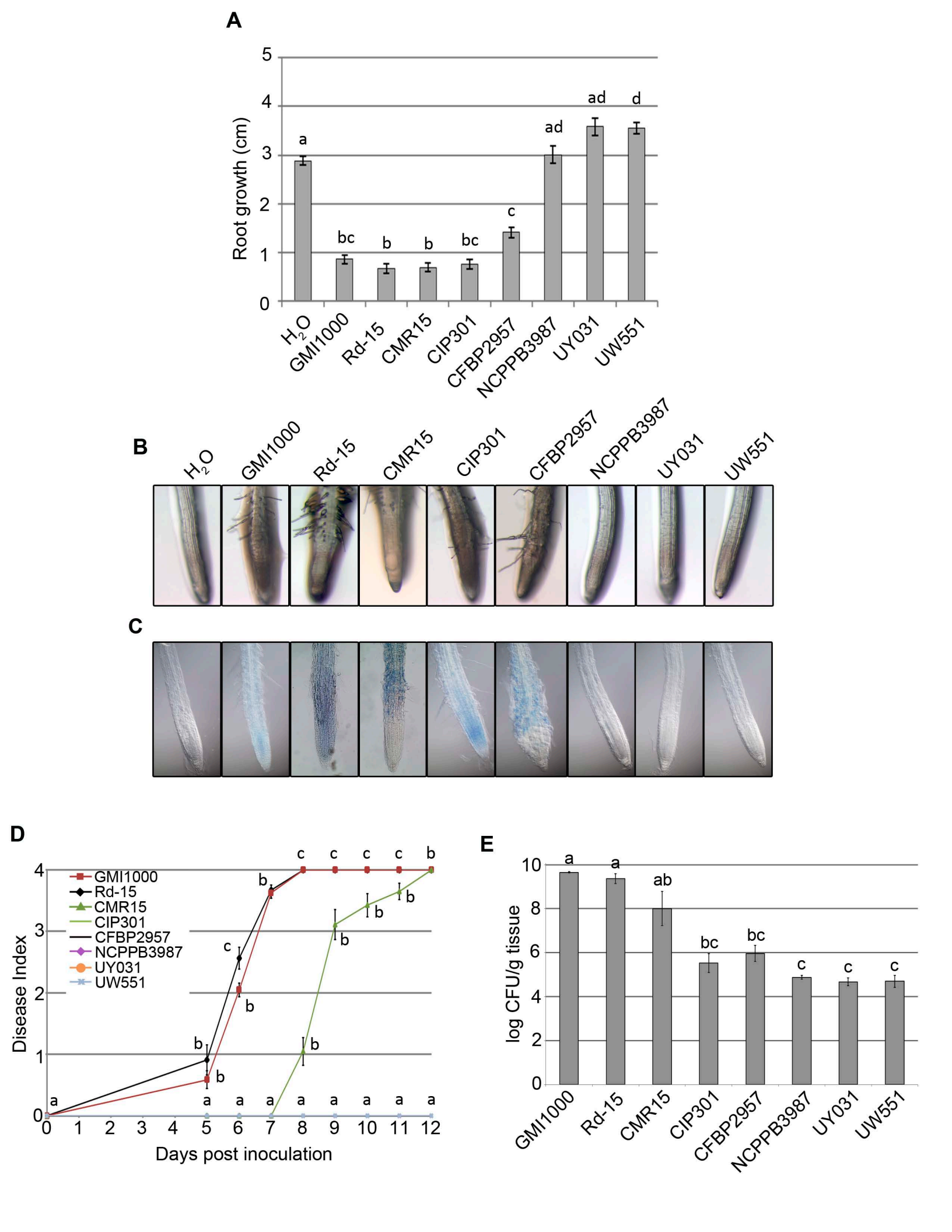
A
Root growth (cm)
0
1
2
3
4
5
a
bc
b
b
bc
c
ad
ad
d
H2O
GMI1000
Rd-15
CMR15
CIP301
CFBP2957
NCPPB3987
UY031
UW551
B
H2O
GMI1000
Rd-15
CMR15
CIP301
CFBP2957
NCPPB3987
UY031
UW551
C
D
Disease Index
Days post inoculation
GMI1000
Rd-15
CMR15
CIP301
CFBP2957
NCPPB3987
UY031
UW551
E
log CFU/g tissue
a
a
ab
bc
bc
c
c
c
GMI1000
Rd-15
CMR15
CIP301
CFBP2957
NCPPB3987
UY031
UW551

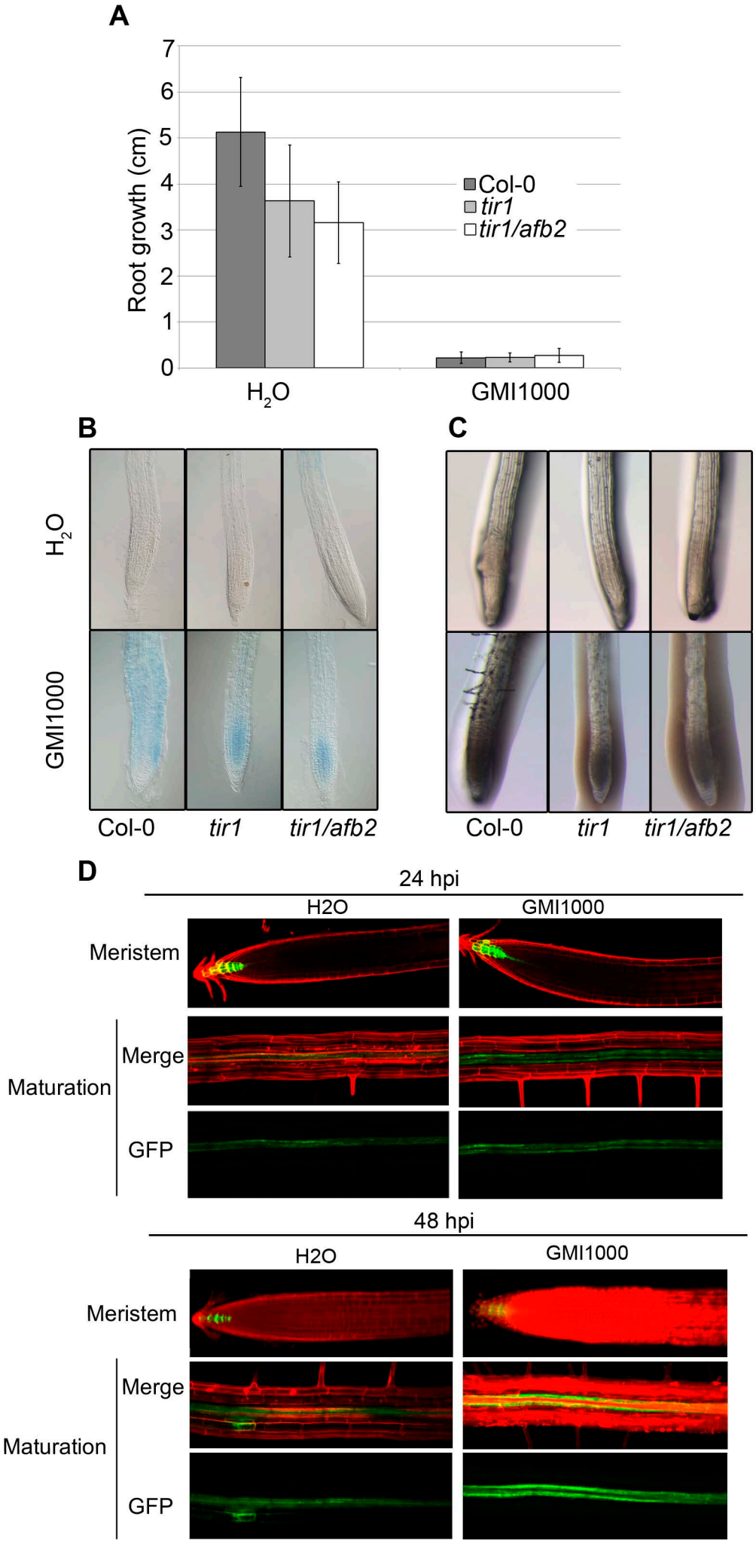
A
Root growth (cm)
0
1
2
3
4
5
6
7
Col-0
tir1
tir1/afb2
H2O
GMI1000
B
C
H2O
GMI1000
Col-0
tir1
tir1/afb2
Col-0
tir1
tir1/afb2
D
24 hpi
H2O
GMI1000
Meristem
Maturation
Merge
GFP
48 hpi
H2O
GMI1000
Meristem
Maturation
Merge
GFP

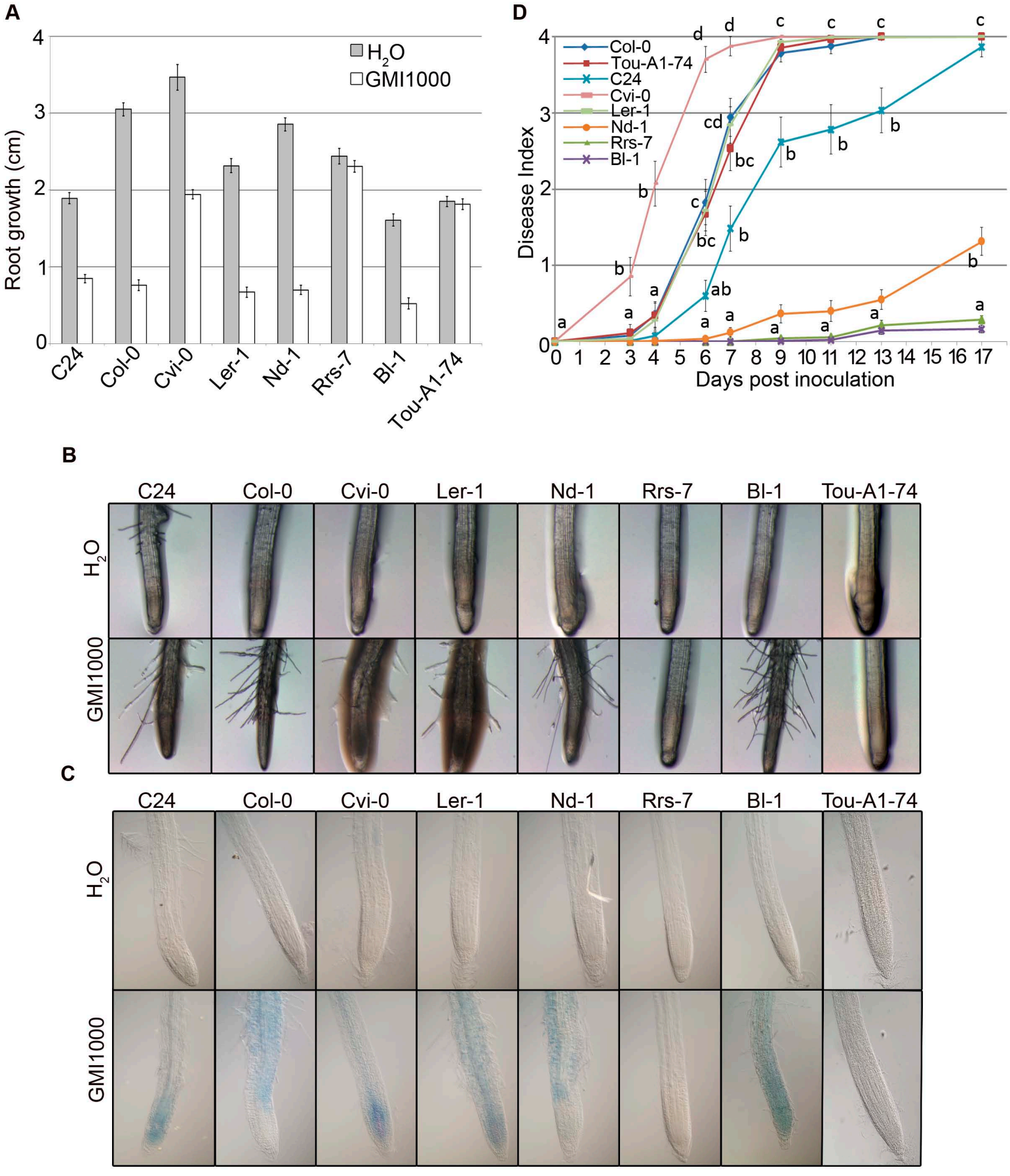
A
Root growth (cm)
H2O
GMI1000
C24
Col-0
Cvi-0
Ler-1
Nd-1
Rrs-7
Bl-1
Tou-A1-74
D
Disease Index
Days post inoculation
B
C
H2O
GMI1000

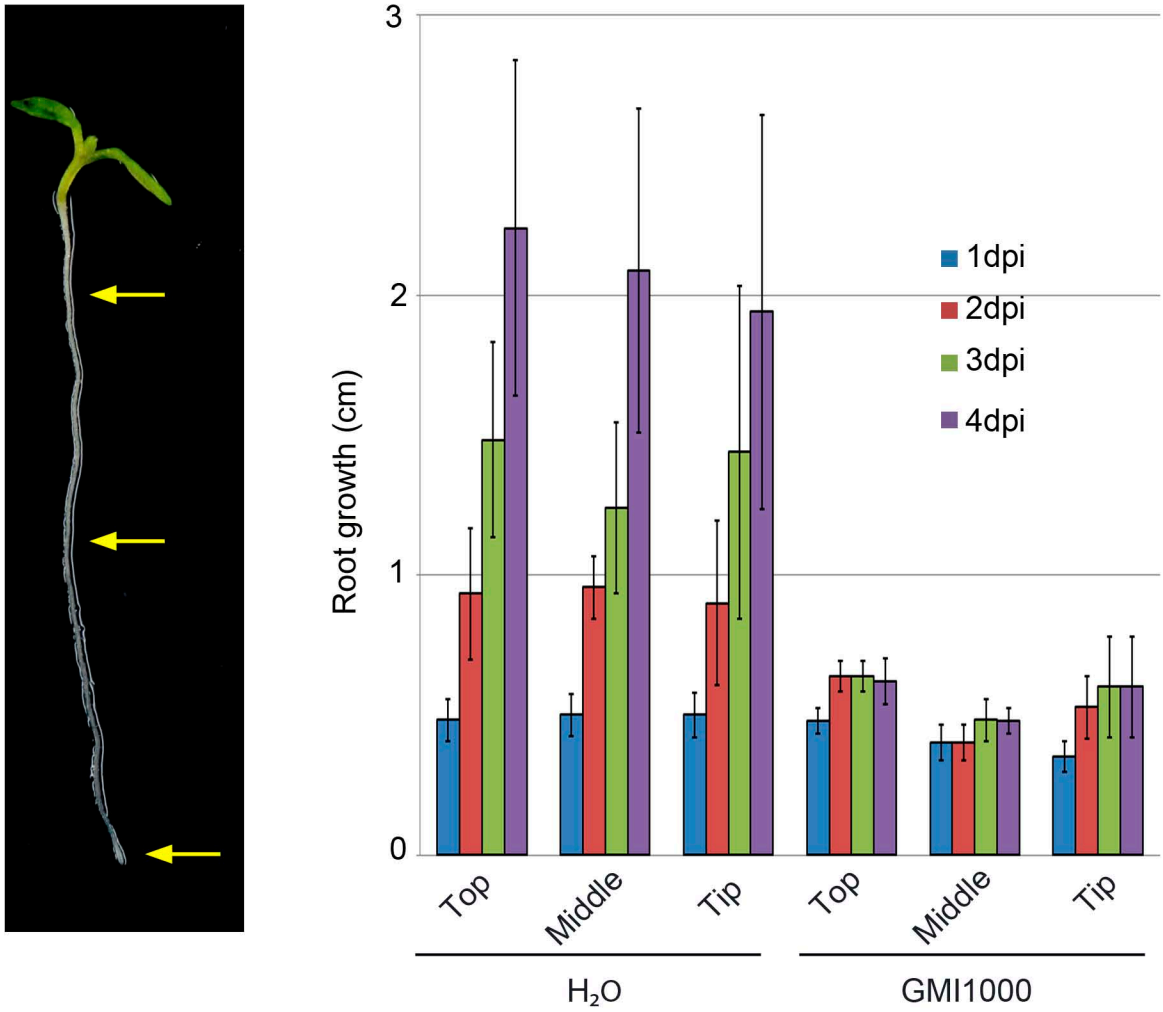

Figure S1. The root site of infection does not have effect on growth inhibition caused by *R. solanacearum* GMI1000. Six-day-old Col-0 seedlings were inoculated with GMI1000 or water. Left panel: Picture of a 6-day-old seedling before infection, with yellow arrows pointing at the selected positions for *R. solanacearum* infection. Right panel: root growth inhibition occurs independently of the site of infection. 5-8 plants were used in at least 3 different experiments

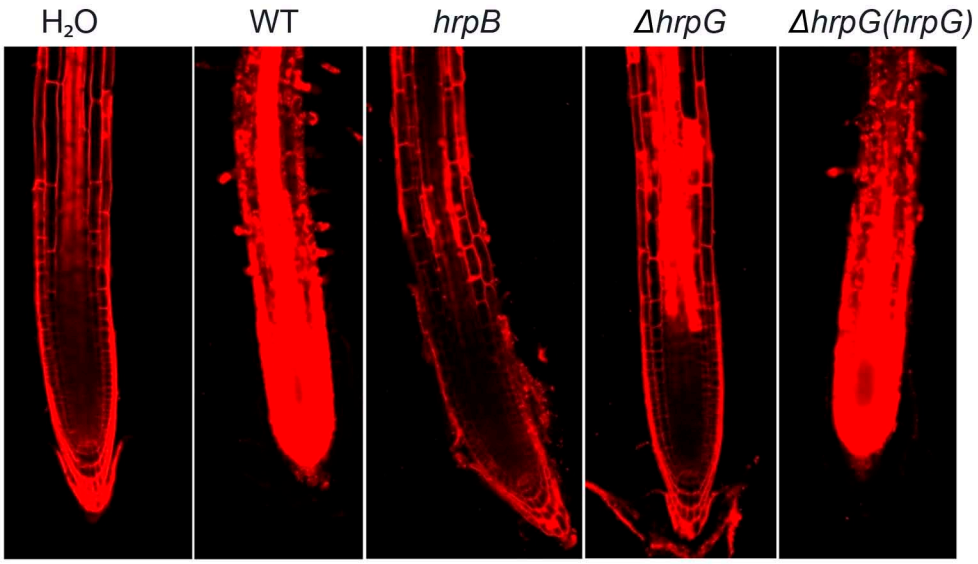

Figure S2. *R. solanacearum*-triggered cell death at the root tip visualized using propidium iodide staining. Photographs were taken using confocal microscopy at 6 dpi.

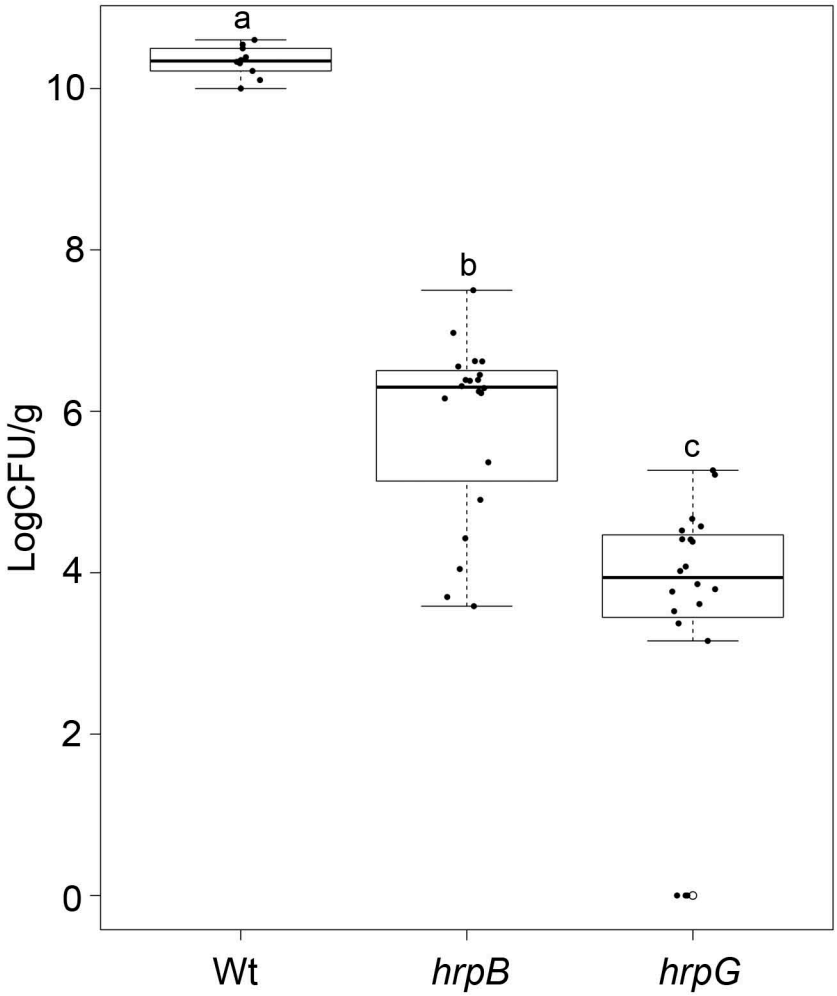

Figure S3. *R. solanacearum* GMI1000 *hrpB* and *hrpG* mutants show different plant colonization capacity compared to Wt. Four-week old plants grown in Jiffy pots were inoculated with the following strains: GMI1000 Wt, *hrpB* (Tn5 transposon insertion) and *hrpG* (Tn5 transposon insertion) at OD600 of 0.01 (10^7 cfu/mL). At 14 dpi bacterial load was calculated; three different experiments are plotted, with a total of 10 plants for the Wt control, 20 plants for *hrpB* and 20 plants for *hrpG*. Letters indicate statistical significance; values not sharing letters represent significant mean differences by post-hoc Tukey´s ($p < 0.05$)

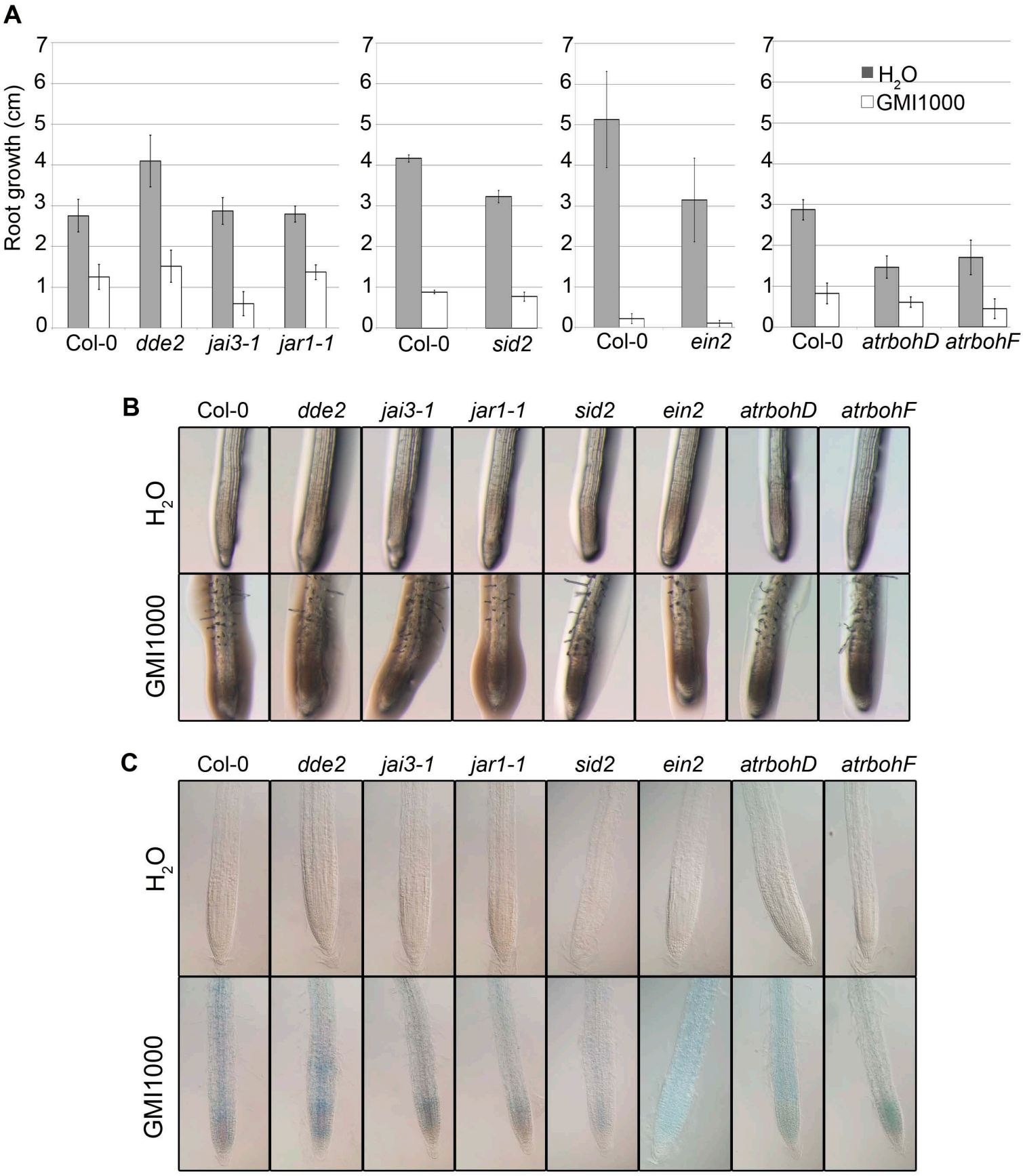

Figure S4. The plant defense regulators jasmonic acid, ethylene, salicylic acid and reactive oxygen species are not essential for the triple phenotype caused by *R. solanacearum* GMI1000 infection. Six-day-old mutant dde2, jai3-1, jar1-1, sid2, ein2, atrbohD, atrbohF and wild type Col-0 seedlings were inoculated with GMI1000 or water. (A) Root growth was measured at 6 dpi. (B) Root hair formation was photographed at 6 dpi. (C) Cell death was observed by Evans blue staining at 6 dpi using Nomarski microscopy. Around 6-10 plants were used in at least 3 different experiments.

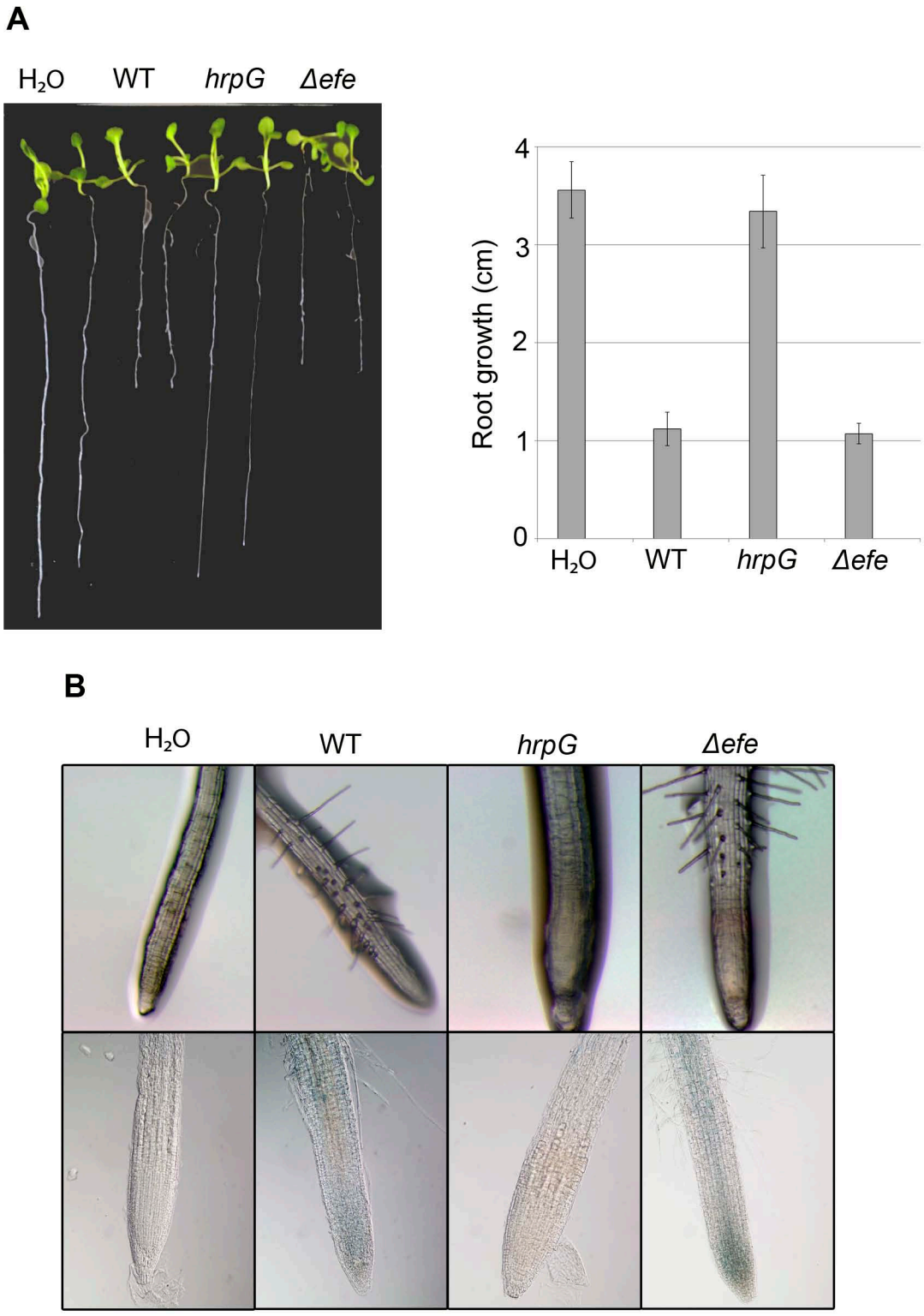

Figure S5. Ethylene produced by GMI1000 is not required for root growth inhibition, root hair formation nor cell death. (A) Disruption of the ethylene forming enzyme gene *efe* does not abolish root growth inhibition and (B) it does not affect root hair formation nor cell death caused by GMI1000. 6-day-old Col-0 seedlings were inoculated with GMI1000 or water. Infected seedlings were photographed at 9 dpi and root growth was measured at 9 dpi. Root hair formation and cell death was stained as in fig. 1 and photographed at 6 dpi. 10-14 plants were used in 3 independent experiments